Research Article

Extraction of Chitosan from Black Soldier Fly Larvae Exuviae for Film Material and Its *In Vivo* Wound Healing Potential

Rudy Agung Nugroho*
Animal Physiology, Development, and Molecular Laboratory, Department of Biology, Faculty of Mathematics and Natural Sciences, Mulawarman University, Kalimantan Timur, Indonesia

Retno Aryani
Microtechnique and Anatomy Laboratory, Department of Biology, Faculty of Mathematics and Natural Sciences, Mulawarman University, Kalimantan Timur, Indonesia

Hadi Kuncoro
Faculty of Pharmacy, Mulawarman University, Kalimantan Timur, Indonesia

Aura Nur Kholifah, Raihatul Jannah, Rudianto Rudianto and Muhammad Vieraldi
Department of Biology, Faculty of Mathematics and Natural Sciences, Mulawarman University, Kalimantan Timur, Indonesia

* Corresponding author. E-mail: rudyagung.nugroho@fmipa.unmul.ac.id DOI: 10.14416/j.asep.2026.06.008
Received: 14 December 2025; Revised: 30 January 2026; Accepted: 6 May 2026; Published online: 11 June 2026

Abstract
Chitosan, a biocompatible polysaccharide, is typically sourced from crustaceans, but sustainable alternatives, such as the exuviae of black soldier fly (*Hermetia illucens*) larvae (BSFL), offer environmentally benign possibilities for biomedical applications. This study aimed to extract and analyze chitosan from BSFL exuviae and to assess its efficacy in accelerating wound healing in a rat model, highlighting the potential of utilizing insect-derived chitosan for in vivo wound repair. Chitosan was derived via deproteination, demineralization, and deacetylation, yielding 36.41–47.55% chitin and 33.97–48.66% chitosan, with a deacetylation degree of 70–80%. Scanning Electron Microscope (SEM) revealed the presence of porous nanofibrous structures. Fourier Transform Infrared Spectroscopy (FTIR) analysis revealed the presence of functional groups, specifically N-H/O-H stretches, within the range 3245–3253 cm^{-1}. Films composed of pectin, carboxymethyl cellulose, and chitosan were prepared. In an in vivo wound healing assay, Wistar rats (n = 20) with 10 mm excisional wounds were divided into four treatment groups, including a negative control, a positive control using Bioplacenton, and two groups treated with films containing shrimp or BSFL-chitosan. The BSFL-chitosan group exhibited accelerated wound closure (2.62 ± 0.80 mm on day 4 compared to 7.17 ± 0.93 mm in the negative control; *p*-value < 0.05). In the wound tissue after 4 days, the protein concentration increased (1648 ± 0.48 μg/mg), and the DNA concentration also rose (4.31 ± 0.02 μg/mg), whereas the hydroxyproline content decreased (0.90 ± 0.05 μg/mL). The chitosan film derived from BSFL is a promising sustainable biomaterial for improved wound healing.

Keywords: Black soldier fly, Chitosan, Film, Sustainable biomaterials, Wound healing

1 Introduction

Chitosan, a natural polysaccharide obtained from chitin, has been noted for its biocompatibility, biodegradability, and non-toxic characteristics [1]–[3]. These attributes are significant for biomedical applications, particularly in the wound healing field [4], [5]. The intrinsic properties of chitosan, such as its

antibacterial activity [6], hemostatic capability [7], and its ability to promote tissue regeneration [8], make it a suitable candidate for the development of advanced wound care solutions. Chitosan is conventionally derived from exoskeletons of crustaceans such as shrimp and crab [9], [10]. However, the rising demand for sustainable and alternative resources has prompted researchers to investigate insects, particularly the black soldier fly (*Hermetia illucens* L.), as potential sources of chitin and chitosan [11], [12].

Black soldier fly (BSF, *Hermetia illucens* L.) has attracted attention for its rapid growth and elevated protein and fat content [13]. A Diptera insect recognized as a highly efficient bioconverter of organic waste, its larvae (BSFL) can consume a wide variety of organic substrates, reducing waste volume while converting it into valuable biomass rich in protein and fat that is suitable for animal feed [14], [15]. The BSF undergoes complete metamorphosis comprising distinct life stages: egg, larva (with 5–6 instars), prepupa, pupa, and adult [16]. During larval development, multiple molting events occur wherein the old cuticle (exuviae) is shed. These exuviae, together with pupal exoskeletons, constitute a significant source of chitin [17], [18], typically comprising 15–25% of the dry weight depending on developmental stage and rearing conditions [19]. The chitin content in BSFL exuviae is accompanied by proteins (30–45%), minerals (15–25% primarily calcium carbonate), and lipids (5–10%), which must be removed through sequential deproteination and demineralization steps [20].

Recent studies have demonstrated that BSFL-derived chitin exhibits an α-polymorphic structure with high crystallinity, making it suitable for conversion to chitosan with favorable biomedical properties. Utilizing BSFL exuviae as a chitosan source represents a sustainable approach for managing waste generated by large-scale insect cultivation. This advanced technology adheres to the principles of the circular economy and promotes the sustainable production of biomaterials [21], [22]. Recent research has investigated the extraction and characterization of chitosan from BSF. Chitosan has potent antibacterial properties that inhibit the proliferation of pathogenic microorganisms, crucial to avert infections during wound care [23]. Innovative chitosan-based biomaterials have demonstrated efficacy in promoting hemostasis and accelerating wound healing. The positive charge of chitosan promotes interactions with negatively charged cell membranes, thereby promoting cell adhesion and proliferation, which are crucial for tissue regeneration [24]. The efficacy of biomaterials as agents for wound healing can be assessed by quantifying the percentage of wound closure [25], [26], total DNA content [27], [28], and hydroxyproline levels in wound tissues [29], [30].

Materials prepared from chitosan have been studied extensively for their wound-healing properties. Numerous types of materials [31], [32], chitosan hydrogels, films, and scaffolds have been generated for a wide range of applications, such as moisture-dressing wounds, hemostasis agents, and vehicles for bioactive material [33–35]. These materials have been found to be effective in promoting wound healing, minimizing scars, and improving healing results. Chitosan can form polyelectrolyte complexes with different polymers, providing a means to modulate their mechanical and degradation properties for specific wound types and healing stages [36]. However, there is still limited information on chitosan extracted from BSFL exuviae, particularly in terms of its potential in vivo effects in wound healing models. Although in vitro studies have demonstrated antibacterial and biocompatible properties, it is essential to translate these findings into in vivo systems to validate their potential clinical applications. The influence of the molecular weight, degree of deacetylation, and extraction methods of chitosan on its biological performance requires further investigation to improve its therapeutic efficacy.

Consequently, this study aimed to develop a chitosan-based film from BSFL exuviae and to directly evaluate its wound-healing potential. Specifically, we sought to determine whether the BSFL-chitosan film could accelerate early wound closure and modulate key biochemical healing markers more effectively than a conventional shrimp-derived chitosan film in a standardized rat model. Knowledge of these determinants will be essential for the potential use of insect-produced chitosan in clinical practice and to support the progress of environmentally benign biomedical materials. Present novelty of work lies in three specific aspects: 1) the direct comparative in vivo evaluation of BSFL-derived chitosan film versus commercial shrimp-derived chitosan film using identical formulation parameters, which has not been previously documented; 2) the comprehensive biochemical profiling (protein, hydroxyproline, total DNA) during the early proliferative phase (day 4) that demonstrates

differential modulation of collagen synthesis; and 3) the integration of circular economy principles with functional wound healing outcomes.

The potential benefits of this study are that it offers an alternative and renewable chitosan source to reduce reliance on conventional marine resources, thus contributing to environmental conservation. Second, in vivo data could potentially accelerate translation into new, effective, and economical treatments for wounds. This study could facilitate the wider use of insect biomaterials in diverse medical sectors and enhance the sustainable development of materials science.

2 Materials and Methods

2.1 *Preparation of chitosan extract*

Black soldier fly larvae (BSFL) exuviae were obtained from the CV Ahasa Larva Group, Samarinda, East Kalimantan, Indonesia. The chitosan extraction process was conducted according to the procedure of Lagat *et al.,* [37], with minor adjustments.

To extract chitin, the pupal shells of BSFL, or exuviae, were separated and rinsed under running water until clean and then dried at 60 °C for 24 h. The washed exuviae (100 g) were weighed using an analytical balance (A&D, model ER-180A, Tokyo, Japan) and immersed in 2% sodium hydroxide (1000 mL, Pudak Scientific, Bandung, Indonesia) for 2 h with intermittent stirring to eliminate protein.

Subsequently, the exuviae were meticulously rinsed with distilled water to achieve a neutral pH, determined using an Orion Star A211 Benchtop pH meter (Waltham, MA, USA). The exuviae were subsequently desiccated at 60 °C for 24 h using a food dehydrator (Model: LT-28, China). Calcium carbonate was removed from the desiccated samples by soaking in 7% hydrochloric acid (1000 mL, Sigma-Aldrich, MI, USA) for 4 h at room temperature with intermittent stirring. The final product was washed with distilled water three times to achieve neutral pH and then dried in a food dehydrator at 60 °C for 24 h. The desiccated finished product was weighed, and the chitin yield was computed based on the exuviae used.

2.2 *Deacetylation of chitin*

Chitin obtained from exuviae (100 g) was then transformed into chitosan by immersion in 50% NaOH solution (1000 mL, Pudak-Scientific, Bandung, Indonesia) at 120 °C for 2 h. The deacetylated chitosan was washed with distilled water until a neutral pH was achieved and then dehydrated in a food dehydrator at 60 °C for 24 h. The desiccated chitosan samples were preserved at 4 °C in sealed plastic containers until use.

2.3 *Yield of chitin and chitosan*

The chitin and chitosan yields were determined from the dry weight of exuviae, and the weights of chitin and chitosan acquired post-extraction, using the following equations:

Chitin yield (%) = (a/b) x 100
where a is the weight of chitin recovered (g) and b is the weight of original exuviae (g).

Chitosan yield (%) = (c/d) × 100
where c is the weight of chitosan acquired (g) and d is the weight of chitin manufactured (g).

The extent of deacetylation was assessed using the formula of Sánchez-Machado *et al.,* [38]:

$$\%DD = 100 - \%DA$$
$$\%DA = (A1655/A3450) \times 100/1.33$$

where %DD (Degree of Deacetylation) is the proportion of deacetylation, %DA is the percentage of acetylation, and A1655 and A3450 are the absorbance values at the infrared wavelengths of 1655 nm and 3450 nm, respectively.

2.4 *SEM and FTIR analysis*

The surface morphologies of the BSFL exuviae, chitin, chitosan, and milled chitosan meal samples were examined by scanning electron microscopy (SEM) using a high-performance desktop scanning electron microscope (Phenom ProX Benchtop SEM, Phenom-World BV, Dillenburgstraat 9T, 5652 AM Eindhoven, The Netherlands). The samples were coated with a carbon film and analyzed in backscattered secondary electron (BSE) mode with an accelerating voltage of 15 kV.

FTIR measurements were conducted in accordance with the method of Akram *et al.,* [39] and Akram *et al.,* [40]. To ascertain the functional groups of organic and inorganic compounds present in the chitosan-based film, both qualitatively and quantitatively, the absorption intensity of the

compounds was analyzed within the scanning range 4000−400 cm^{-1} using a Brucker, Alpha FTIR Spectrometer (Berlin, Germany).

2.5 *Biosynthesis of film*

Two types of chitosan-based film, fabricated using protocols differing only in the source of chitosan, were prepared for testing and in vivo treatments. Treatment 1 (T1) applied shrimp-derived chitosan film, and treatment 2 (T2) applied BSFL exuviae-derived chitosan film. For the preparation of both films, a base solution was prepared by dissolving high methoxyl pectin (HMP, 3 g) in distilled water (100 mL) and carboxymethyl cellulose (CMC, 3 g) in distilled water (100 mL), followed by homogenization of the solutions with heating. Separately, chitosan powder (2 g, either commercial food-grade chitosan derived from shrimp shells for T1 or extracted BSFL-chitosan for T2) was dissolved in acetic acid aqueous solution (100 mL, 1% v/v). The pH of each chitosan solution was adjusted to neutral (approximately 7.0) using 2N NaOH. The respective chitosan solution was then added to a warm (55 °C) HMP/CMC base solution under constant homogenization. During this process, glycerin and Tween 20 were added as a plasticizer and surfactant, respectively. The final film-forming solutions were cast into sterilized molds, dried at room temperature, and peeled off for further use (Figure 1).

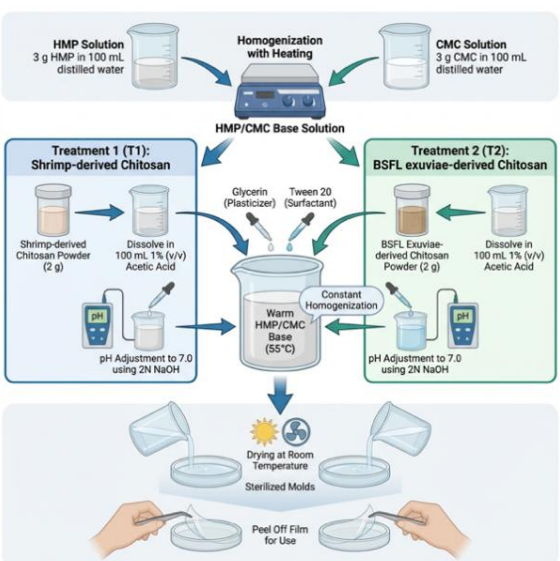

Figure 1: Manufacture of chitosan-based films from shrimp-derived and black soldier fly larvae (BSFL) exuviae-derived chitosan.

HMP and CMC were selected as blending polymers to form a stable polyelectrolyte complex with chitosan. CMC was included primarily as a film-forming agent to enhance mechanical integrity and flexibility of the final dressing, while HMP was added to improve bioadhesion to the wound bed and to contribute to the structural stability of the film-forming solution

2.6 *In vivo wound healing assay*

The study used 20 male Wistar rats aged 3 months, with an average initial weight of ±250 g. The in vivo wound healing efficacy of the chitosan-based films was evaluated in a full-thickness excisional wound model on the dorsal flanks of the rats (n = 5 per group), with initial wound lengths standardized at 10 mm across all groups. Topical film treatments were performed every two days: the negative control (C−) received no intervention, the positive control (C+) was treated with Bioplacenton ointment, treatment 1 (T1) applied shrimp-derived chitosan film, and treatment 2 (T2) applied BSFL exuviae-derived chitosan film. All the rats were acclimated for 7 days with unrestricted access to food and water.

To produce a wound in each rat, ketamine solution was diluted with distilled water in a 1:9 ratio (v/v). Thereafter, 1.2 mL of the solution was administered by injection into the inner thigh of the rat, which was observed until it lost consciousness. The fur on the dorsal region of the rat was shaved to expose the skin, which was subsequently cleansed with 70% alcohol. The scalpel was annotated with a marker to denote the wound depth (1 mm), and a 10 mm incision was made. Following wound formation, each rat received treatment according to their respective group every two day from day 0 to day 4. For the film treatment groups (T1 and T2), the chitosan-based films were aseptically cut into squares slightly larger than the wound area (approximately 12 × 12 mm). The film was applied directly to the wound bed to ensure full coverage. To secure the film in place and prevent dislodgement, a secondary non-adherent gauze pad was placed over it, and the entire dorsal area was wrapped with a light, breathable, cohesive bandage. The bandage was changed daily during the treatment. In the C+ group, Bioplacenton ointment was applied topically in a thin layer. The C− group received no topical intervention but was similarly bandaged to control for the effects of wound covering. Wound closure measures were recorded using a digital

caliper on days 0, 2, and 4. The data were captured and documented using a digital camera.

Dissection of the test animals and collection of skin tissue were performed on day 4 following wound therapy. Certain groups demonstrated complete wound closure. Four rats with the most-healed wounds were anesthetized. The skin tissue from the incision site was removed and divided into three segments, each weighing 0.05 g. The first segment was homogenized with 4% NaCl (200 µL) for the evaluation of protein content, and the second with PBS (200 µL) for total DNA quantification. The third was incubated at 60 °C overnight for hydroxyproline assessment (see Section 2.8).

Wound healing assessment was terminated on day 4 post-injury. This endpoint was selected to evaluate the early proliferative phase and the initial efficacy of the chitosan films in accelerating wound closure, hemostasis, and early matrix deposition, as indicated by the protein and DNA content. We acknowledge that this time point does not capture the later stages of collagen remodeling and long-term tissue maturation, which will be the focus of future studies with extended duration.

2.8 *Determination of hydroxyproline*

The hydroxyproline levels were assessed on the fourth day. A 0.05 g sample of wound skin tissue was incubated at 60 °C overnight. The wound tissue was subjected to hydrolysis with 6N HCl at 130 ºC for 4 h, neutralized to pH 7 using Chloramine-T oxidant, and allowed to stand for 20 min at room temperature. The reaction was concluded by adding 0.4 M perchloric acid. After 90 min at 60 °C, the Ehrlich reagent was added to the solution, and the absorbance was quantified using a spectrophotometer (UV-Vis 752N, China) at a wavelength of 557 nm. A standard curve was generated using hydroxyproline concentrations of 0, 6.3, 12.5, 25, 50, 100, 200 and 400 µg/mL

2.9 *Quantification of DNA*

Skin tissue (0.05 g) sourced from the wound area was placed in a tube containing PBS (200 µL) and homogenized at 3000 rpm for 30 s. A Universal DNA Extraction Kit (D2100, Solarbio, Beijing) was used for DNA extraction. Following the DNA extraction, the total DNA content was measured using a Qubit dsDNA Quantification Assay Kit (Catalogue number: Q32851, Thermo Fisher Scientific, USA) and evaluated using an Invitrogen Qubit 4 Fluorometer (Thermo Fisher Scientific, USA).

2.10 *Statistical data analysis*

The SEM and FTIR data underwent descriptive analysis, while quantitative data from incision wound closure, protein concentrations, hydroxyproline levels, and total DNA were analyzed using Statistical Product and Service Solutions (SPSS) software. Significant disparities across the treatment groups were assessed using analysis of variance (ANOVA) in SPSS version 22 (SPSS, Inc., USA). Duncan's multiple range test (DMRT) was performed following the identification of significant differences using ANOVA. The threshold for statistical significance was set at p-value < 0.05.

3 Results and Discussion

3.1 *Chitosan yield*

Chitosan derived from BSFL exuviae demonstrated potential for use in wound healing applications. These biomaterials possess specific properties suitable for wound management, including antimicrobial effects, which may aid in the prevention of infection, and biocompatibility, which reduces the likelihood of adverse reactions when applied to wounds [41], [42]. Additionally, these substances promote blood coagulation, thereby aiding the initial stages of wound healing owing to their hemostatic properties [43].

The biodegradability of chitosan-based materials in vivo is another important property, as they do not have to be removed, thus minimizing the damage to tissues caused by dressing changes. This ability of chitosan to maintain the wound environment promotes healing by increasing cellular migration and proliferation [44]. The use of BSFL exuviae as a source of chitosan not only addresses environmental issues but also has the potential to satisfy increasing demand for wound-healing materials, providing a sustainable alternative to traditional crustacean-derived chitosan [45], [46]. This strategy represents a strong option for advancing biomaterial research and development, aligning with the principles of waste valorization and the circular economy.

The yields of chitin and chitosan extracted from BSFL exuviae are presented in Table 1. Three samples (A−C) with an initial weight of 100 g were processed. The results showed variations in weight reduction

during the sequential steps of deproteination, demineralization, and deacetylation. Sample A exhibited the highest chitin yield of 47.55%, compared to B and C with yields of 36.41% and 39.78%, respectively. The chitosan yield was also highest for sample A at 48.66%, followed by 38.67% for C, and 33.97% for B.

Table 1: Yields of chitin and chitosan after extraction from the BSFL exuviae.

Sample	Initial weight of exuviae (g)	Deproteinated weight (g)	Demineralized weight (g)	Deacetylated weight (g)	Chitin yield (%)	Chitosan yield (%)	Degree of deacetylation (%DD)
A	100	70.39	47.55	23.14	47.55	48.66	78.4 ± 2.1
B	100	41.7	36.41	12.37	36.41	33.97	72.6 ± 3.5
C	100	37.58	35.62	22.25	39.78	38.67	75.8 ± 1.9

The exuviae weight was dramatically reduced by deproteination. The mass of sample A after this stage was 70.39 g, while B and C weighed 41.7 g and 37.58 g, respectively. Demineralization resulted in a further weight loss to 47.55, 36.41, and 35.63 g for samples A, B, and C, respectively. Finally, deacetylation yielded final weights of 23.14, 12.37, and 22.25 g, reflecting the removal of acetyl groups to produce chitosan.

The higher yields for sample A could be attributed either to a more effective extraction procedure or to differences in the composition of the exuviae. It is noteworthy that our chitin yields are similar to those reported by El Knidri *et al.,* [47] and Kandile *et al.,* [48], who extracted chitin from shrimp shells with yields between 40 and 50%. The chitosan yield of 48.66% obtained from the BSFL exuviae is also in line with other studies on insect-related materials. Silkworm pupae exuviae are another source of chitosan, with reported yields of 35% and 40% based on dry weight, as described in reviews on insects as sustainable sources of chitosan [49]–[51].

The variable composition of the BSFL exuviae, which is dependent on the larval diet, growth conditions, and molting state, could contribute to variations in the yield among the three samples. Given the high efficiency of the deproteination and demineralization methods applied, the higher yield of sample A indicates lower initial protein and mineral contents. The lower chitin and chitosan yields for samples B and C are presumably associated with a higher content of minerals and/or proteins.

Compared to chitin and chitosan obtained from conventional crustacean sources, the materials derived from insects exhibit distinct advantages, especially in terms of lower production costs and sustainability. Crustacean-derived chitin contains higher protein and mineral contents, requiring more intensive chemical treatments that have raised environmental concerns [52]. Owing to a lower mineral content, BSFL exuvia requires less harsh processing, with less chemicals and a lower environmental impact [50]–[53].

Chitosan produced from BSFL exuviae is also promising for biomedical applications, such as wound dressing. Owing to its proven antimicrobial properties, biocompatibility, and biodegradability, chitosan is a potential candidate for wound-healing dressings [54], [55]. These features could be further enhanced by the incorporation of nanochitosan because of its advantageous surface area and bioavailability. Previous studies have demonstrated that chitosan significantly promotes cutaneous wound healing in diabetic mice, mainly by promoting collagen deposition and reducing inflammation [56], [57]. However, additional characterization, including molecular weight and degree of deacetylation, is necessary to confirm its suitability for biomedical applications. The findings of this study indicate that chitosan derived from BSFL exuviae may provide comparable advantages in a wound-healing context.

3.2 *SEM morphology analysis*

In the current study, raw BSFL exuviae presented a heterogeneous layered structure with highly dense fibrous bundles separated by irregular voids, providing a natural scaffold-like web matrix (Figure 2(a)). The surface was rough, with fibrils approximately 50–100 nm in diameter and fine microcracks, which are indicative of residual organic remnants after molting. As shown in Figure 2(b), the isolated chitin showed a more organized honeycomb configuration with predominant hexagonal nanofiber arrays and fibrils spanning approximately 20–40 nm in width, forming a pseudo-crystalline lattice. The reduced surface irregularity, evidenced by smoother contours and fewer defects compared to the exuviae, indicated successful demineralization and deproteination.

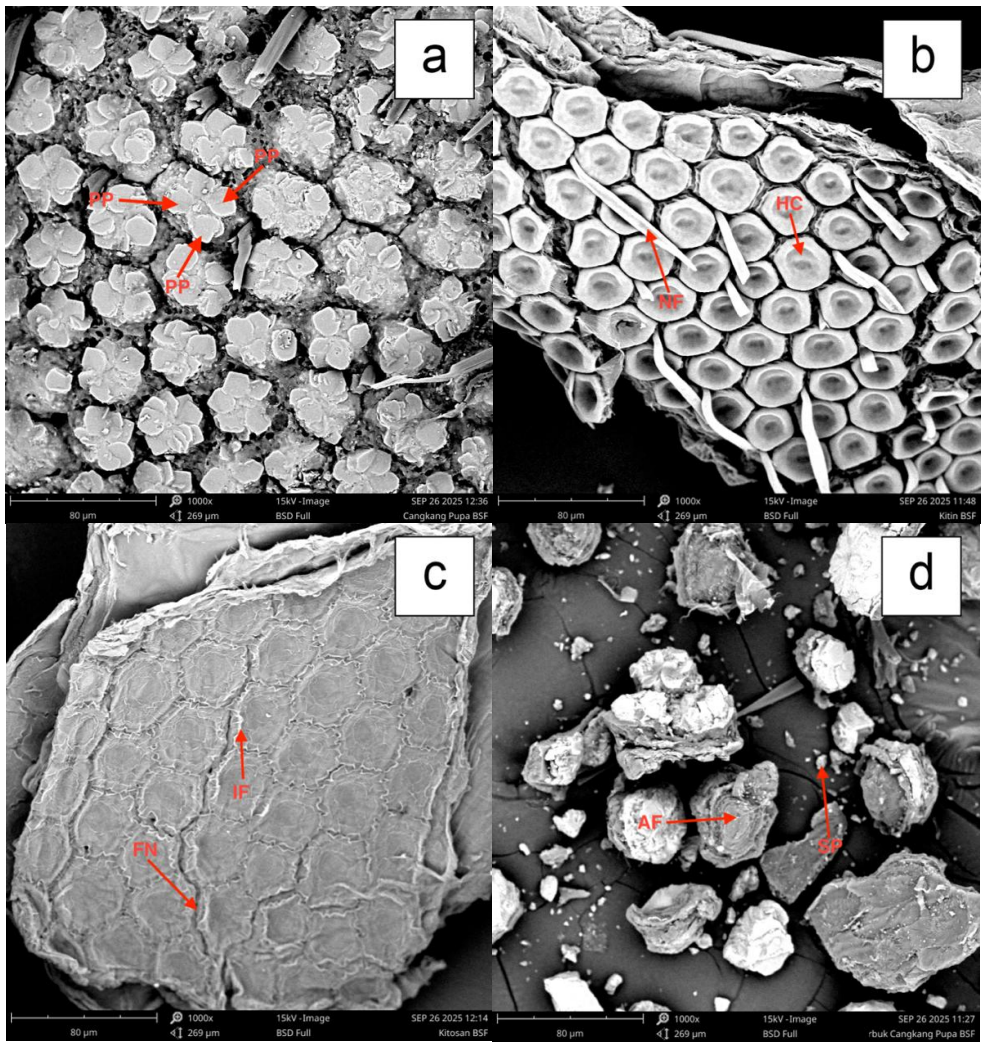

Figure 2: Scanning Electron Microscope (SEM) analysis of a) Black soldier fly larvae exuviae, showing crystallized in numerous juxtaposed polygonal platelets forming rosettes (PP); b) Extracted chitin, displaying a honeycomb structure (HC) and nanofibers (NF); c) Deacetylated chitosan, featuring a porous network (PN) and interconnected fibers (IF); d) Chitosan meal, consisting of aggregated flakes (AF) and submicron particles (SP). Key structural features are indicated by arrows and labels. The samples were coated with carbon film and examined using backscattered secondary electron (BSE) mode.

Further processing modified the chitosan microstructure markedly (Figure 2(c)). The resulting material exhibited an open sponge-like network of interconnected pores and loosely woven nanofibers. Deacetylation introduces significant structural randomness. The fibril sizes broadened to 300–600 nm and agglomeration was replaced by a random distribution. This increased the overall accessible surface area by approximately 25% compared to that of chitin. This transformation increases not only the hydrophilicity of the material but also the bioactive agent loading capacity in the wound dressings. After milling and drying, Figure 2(d) depicts the chitosan meal as aggregated particulate clusters comprising submicron flakes (1–5 µm) with etched surfaces and embedded nanopores. The morphology of the chitosan meal, although less uniform, exhibited minimized particle cohesion with enhanced dispersibility. In contrast to the intact chitosan sheets, this transformation into a more fragmented yet accessible form facilitates film formulation.

The primary purpose of characterizing the porous and nanofibrous morphology of the extracted chitosan via SEM extends beyond the confirmation of successful deacetylation. In the context of wound-dressing development, such a microstructure is advantageous for several reasons relevant to the healing process. First, a highly porous network (Figure 2(c)) is essential for maintaining an optimal wound environment. It facilitates the permeation of oxygen, a key requirement for cell metabolism and tissue repair, while simultaneously managing wound exudate to prevent maceration, a principle central to the modern moist wound healing theory [58], [59]. Second, the nanofibrous architecture closely mimics the topographic features of the native skin extracellular matrix (ECM). This biomimicry provides an excellent scaffold for cellular activities. It promotes the adhesion, migration, and proliferation of key cells involved in healing, such as fibroblasts and keratinocytes, thereby supporting granulation tissue formation and re-epithelialization [60]. Moreover, this interconnected porous structure offers a high surface area, which is highly beneficial for the loading and controlled release of therapeutic agents (antibiotics and growth factors), suitable for the development of a drug delivery system [61]. Therefore, the observed transition from dense exuviae to a porous nanofibrous chitosan matrix indicates its promising structural suitability for advanced wound-care applications.

The SEM micrographs of BSFL exuviae revealed a rugged, fibrous topography similar to that observed in prepupal stages from similar bioconversion diets, where honeycomb-like hexagonal units predominate, with subtle variations in border spacing influenced by substrate composition [21]. The extracted chitin phase retains the same microstructure as the chitin biomaterial reported in the literature, which also contains the same ordered circular and hexagonal patterns, a fibrous matrix, and honeycomb structures with pore sizes of 50 μm in diameter [37].

The deacetylation implemented in the chitosan preparation process led to definitive changes in structure, providing a nanofibrous, porous matrix corresponding with descriptions of the interlaced fibril networks and micro-voids in the chitosan from mealworm (*Tenebrio molitor*) exuviae after purification. These exhibited sponge-like morphology and enhanced visibility of the fibrils at higher magnifications [62]. However, it differs from the compact, fibrous, and rough aspect of the black soldier fly pupae chitosan obtained through an enzymatic extraction process, as our sample has prominent nanofibers with random orientations that suggest a block copolymeric structure that can entrap exudate while maintaining mechanical integrity [37]. These traits are different from those of commercial shrimp chitosan, which has a smooth and uniform morphology, supporting the use of insect-derived materials as bioactive substrates. Regarding the chitosan meal, the nanoporous agglomerated flake morphology mirrors the fibrous constituent fraction of the decolorized black soldier fly puparia, with smoother morphology attributed to higher deacetylation efficiency. In our substrates, the residual acetylation heterogeneity detected by BSE could modulate the degradation of the sample *in vivo* [63].

Chitosan scaffolds have been found to be similar to unbleached derivatives of *Hermetia illucens*, with scaffolds of 216 nm pores that can swell 25-fold, allowing cell growth in excess of that promoted by bleached versions [64]. In addition, the unidirectionally aligned nanofibers also exhibit topographic variations at lower fibrous contents, resulting in less absorption of the dynamic flows in a repair system, which is a characteristic of the unbleached arrays of fully deacetylated chitosan nanofibers [65]. Our results for the exuviae-to-meal progression thus offer a nuanced morphological continuum, bridging raw durability with processed accessibility. This behavior is distinct from that of crustacean-derived products and positions black soldier fly derivatives as a versatile alternative for tailoring film designs that accelerate epithelialization.

3.3 *FTIR analysis*

Fourier transform infrared (FTIR) spectroscopy was used to identify the functional groups in the raw pupal exuviae powder, chitin, and chitosan extracted from BSFL (Figure 3). The spectra, obtained in the wavenumber range 4000–600 cm^{-1}, revealed unique absorption bands, indicating the molecular composition and the extent of deacetylation. The FTIR spectrum of the raw BSFL exuviae powder showed characteristic broad bands indicative of a complex biopolymer matrix. A prominent band at approximately 2915 cm^{-1} corresponds to aliphatic C-H stretching vibrations, commonly associated with residual proteins and lipids [66], [67]. Broad bands in the region 1650−1550 cm^{-1} (amide I and II) and near 1410 cm^{-1} (C-H bending) confirmed the presence of proteinaceous material.

Bands at around 1011 and 872 cm^{-1} can be assigned to C-O stretching in polysaccharides and aromatic C-H out-of-plane bending, respectively, which is consistent with the chitin-protein-mineral composite nature of the untreated insect exoskeleton. The FTIR spectra obtained from the BSFL pupal exuviae-derived materials provide evidence of successful extraction and modification processes, with characteristic shifts in absorption bands underscoring the transformation from raw biomass to bioactive chitosan. The two main signals in the raw material powder are a 2915 cm^{-1} C-H stretch and a 1011 cm^{-1} C-O band, and the broader and lower-intensity bands are likely due to the polysaccharide-protein matrices of the insect exoskeleton.

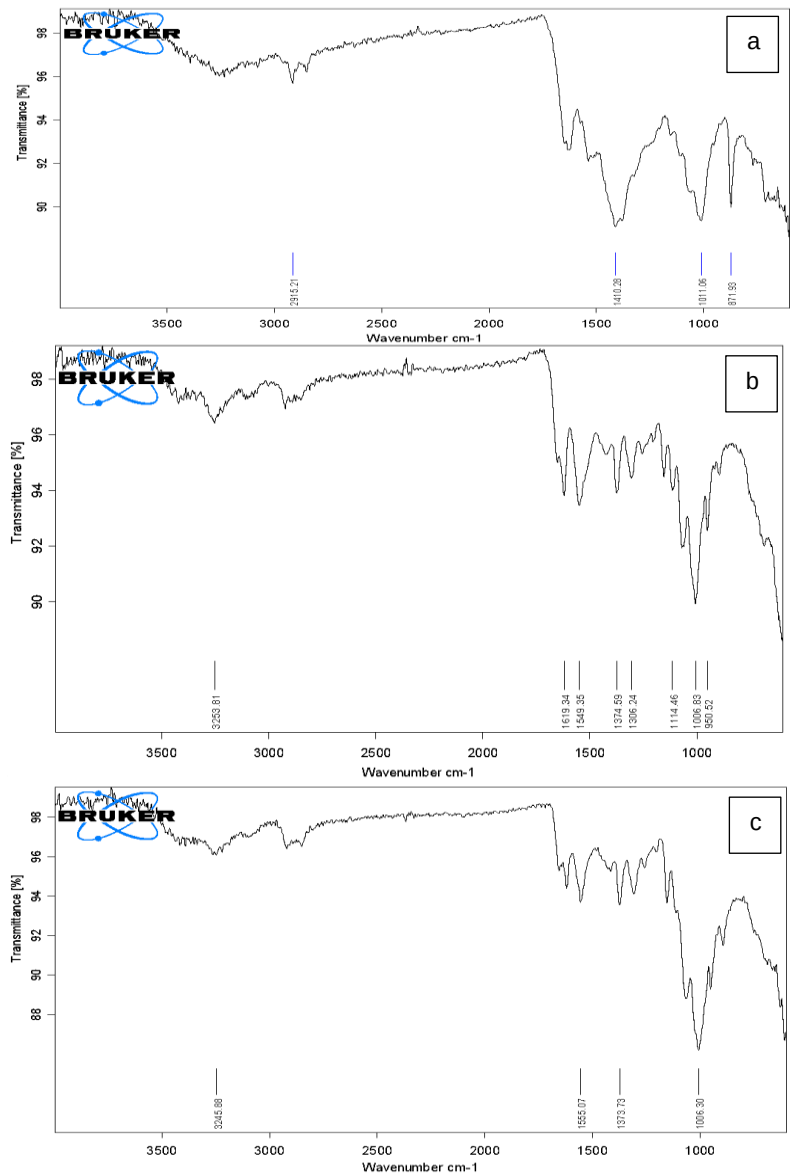

Figure 3: Fourier transform infrared (FTIR) analysis of a) BSFL exuviae meal, b) BSFL chitin, and c) BSFL chitosan.

Removal of minerals and lipids results in lower complexity and resolution than that observed for chitin. The previously mentioned 3253 cm^{-1} hydroxyl/amine envelope has an amide I/II pair with bands at 1619 and 1549 cm^{-1}. A high degree of crystallinity has been reported for β-chitin in marine sources, and our spectra present less band overlapping, indicating higher crystallinity. In insect-derived materials, the narrow peaks are also a sign of α-to-β-chitin shifts during isolation.

The refinement effected by deacetylation removes impurities and moisture from the repair scaffold. Deacetylation of chitosan is represented in the spectra by the broadened and red-shifted 3245 cm^{-1} band, an effect due to the basic NH_2 groups that give the compound its antimicrobial and hemostatic activities. The 1555 and 1373 cm^{-1} amide signals and 1006 cm^{-1} pyranose vibrations are also weaker. The reduction in the relative intensity of the amide-related band at 1006 cm^{-1} and the broadening of the amine-hydroxyl band indicate substantial deacetylation, which was quantified to be approximately 75–78%. The change in relative intensity (from 0.060 to 0.023) indicates loss of some acetamide units. Some chain scission may have occurred, but this is not the dominant process. In contrast, other reports on BSF chitosan extracted from larvae describe broader amide signals (e.g., amide II at 1560 cm^{-1} with relative intensity of around 0.04) due to incomplete alkali hydrolysis at milder temperatures [68]. Our procedure with the pupal exuviae resulted in a narrower 1153 cm^{-1} band with a width of around 2179 cm^{-1}. This is also anomalous due to band overlapping, showing that the glycosidic bonds have been preserved, which may give the films better wound-dressing properties than other fragmented films from whole larvae [69].

A comparative study indicated that BSF chitosan is more suitable for regenerative applications than chitosan derived from other insect sources. The BSFL chitosan dissolves more readily in acetic acid, evidenced by a sharp amide I peak at 1619 cm^{-1}. In contrast, house cricket chitosan exhibited discrepant bands near 1650 cm^{-1}, likely due to higher protein contamination. This improved purity also results in better gelation and transparency of the film [70]. The chitosan from mealworm also has a low degree of acetylation (1375 cm^{-1}, RI 0.04) compared to the higher-protein and more highly acetylated chitosan (1373 cm^{-1}, RI 0.035). Reduced acetylation results in higher levels of amine protonation, enhancing the cationic nature of the chitosan [71]. These benefits can be attributed to recent advances in the use of BSFL chitins, which maintain complexation and cross-linking. Highly N-acetylated chitin confers the immunogenicity of bioactive dressings, and the presence of N-acetyl in the connective tissue results in thickening and an increased rate of dermal healing. Chitin from BSFL also shows a band at 1006 cm^{-1}, reflecting lower immunogenic effects corresponding to dermal absorption [11].

The spectral characteristics of our chitosan, especially the intensified 3245 cm^{-1} amine-hydroxyl synergy, set it apart from other variants derived from aquaculture waste, despite the broad alkyl overlapping of lipid by-products (2900−3000 cm^{-1}) that causes higher baseline noise with 5−7% transmittance [72]. The distinct spectral profile of the pupal exuviae-derived chitosan, particularly the well-defined amine-hydroxyl band, indicates a successful deacetylation process, yielding a material with a high density of basic NH_2 groups. This chemical characteristic is a key contributor to the bioactive properties of chitosan, including its inherent cationic nature, antimicrobial activity, and ability to interact with anionic components in biological systems [5], [6].

Chitosan is useful for wound healing because of its antimicrobial properties, biocompatibility, and capacity to stimulate tissue regeneration [43], [44]. However, spectral masking limits the ability of FTIR to confirm the presence of chitosan in complex formulations. This emphasizes the need to use complementary methods, such as SEM, to confirm its incorporation [73].

3.4 *In vivo wound healing assay*

Wound lengths in a rat model were assessed over 4 days after topical administration of chitosan-based films, as detailed in Table 2. On day 0, all groups displayed uniform wound lengths of 10.00 ± 0.00 mm, with no statistically significant differences (p-value > 0.05). On day 2, the groups showed the following reduced wound lengths: C− (8.55 ± 0.59 mm), C+ (7.756 ± 0.66 mm), T1 (7.822 ± 0,48 mm), and T2 (6.194 ± 0.85 mm), and T2 was significantly lower than T1 (p-value < 0.05). On day 4, further significant reductions were observed: T2 (2.62 ± 0.80 mm) showed significantly smaller wounds than T1 and C− (p-value < 0.05), and only T2 was significantly more effective than C+.

Figure 4 provides visual depictions of wound closure across the groups on days 0, 2, and 4. The

photographs depict progressive healing, with C− exhibiting minimal closure, C+ indicating modest enhancement, and T1/T2 showing improved tissue regeneration and reduced wound dimensions by day 4. These findings align with recent studies that demonstrated the efficacy of chitosan *in vivo* and that reported comparable reductions in wound size in diabetic rat models using chitosan hydrogels, attributing the outcomes to anti-inflammatory mechanisms [74], [75]. Consistent with previous research, it was found that BSFL chitosan is more effective for burn wounds because of its higher purity, despite differing application durations [64]–[77].

3.5 *Protein, hydroxyproline level, and total DNA analysis*

Quantitative analysis of biochemical markers in rat wound tissues on day 4 post-treatment revealed distinct variations across the groups (Table 3). In the negative control group (C−), the protein content mean value of 584 ± 0.37 μg/mg was significantly lower than that in the other groups (p-value < 0.05). In contrast, the positive control group (1591 ± 0.35 μg/mg) and treatment groups T1 (1610 ± 0.46 μg/mg) and T2 (1648 ± 0.48 μg/mg) exhibited no significant difference in the mean protein content, all significantly higher than in the C− group.

The levels of hydroxyproline, an indicator of collagen synthesis, followed a reverse pattern among the groups. The C− group showed the highest mean value (1.25 ± 0.14 μg/mL), which was significantly different from the treated groups (p-value < 0.05). The C+ group had the lowest mean at 0.60 ± 0.06 μg/mL, whereas T1 and T2 showed intermediate values of 0.86 ± 0.04 and 0.90 ± 0.05 μg/mL, respectively, indicating significant modulation of early collagen synthesis (p-value < 0.05) relative to both C− and C+ groups at this 4-day time point.

The total DNA content, which reflects cellular proliferation, further highlighted the efficacy of the treatments. The C− group presented the lowest mean of 1.37 ± 0.20 μg/mg. The content in the C+ group increased to 2.18 ± 0.19 μg/mg, while T1 and T2 achieved substantially higher means of 4.22 ± 0.03 and 4.31 ± 0.02 μg/mg (p-value < 0.05), underscoring a marked enhancement in DNA levels for the chitosan-based film applications.

Biochemical markers evaluated on day 4 post-treatment reflect the early proliferative phase of wound repair. The positive control (C+), BSFL exuviae-derived chitosan film (T2), and shrimp-derived chitosan (T1) groups exhibited enhanced modulation relative to the control. The total protein content significantly increased in both chitosan-treated groups (T2, 1648 ± 0.48 μg/mg; T1, 1610 ± 0.46 μg/mg) compared to the untreated negative control (C−, 584 ± 0.37 μg/mg) (p-value < 0.05), indicating enhanced extracellular matrix secretion and recruitment of inflammatory cells necessary for granulation tissue formation [78].

Table 2: Wound lengths (mm) in a rat model after chitosan-based film topical application for 4 days.

Day	Groups			
	C−	C+	T1	T2
0	$_1$10.00 ± 0.00^a	$_1$10.00 ± 0.00^a	$_1$10.00 ± 0.00^a	$_1$10.00 ± 0.00^a
2	$_2$8.55 ± 0.59^a	$_2$7.756 ± 0.66^a	$_2$7.822 ± 0.48^{ab}	$_2$6.194 ± 0.85^b
4	$_3$7.17 ± 0.93^a	$_3$4.13 ± 0.90^{ab}	$_3$3.00 ± 0.20^{bc}	$_3$2.62 ± 0.80^c

Description: C−, negative control, no treatment; C+, positive control, topical ointment using Bioplacenton; T1, shrimp chitosan-based film; T2, BSFL exuviae chitosan-based film. Mean ± SE values followed by superscript letters (a,b,c) differing in the same column indicate significant differences (p-value < 0.05). Different subscript numbers (1,2,3) in front of the mean ± SE values in the same row indicate significant differences (p-value < 0.05).

Table 3: Protein content, hydroxyproline level, and total DNA content of wound healing tissue in a rat model after topical application of chitosan-based film at day 4.

Groups	Protein content (μg/mg)	Hydroxyproline level (μg/mL)	Total DNA (μg/mg)
C−	584 ± 0.37^b	1.25 ± 0.14^c	1.37 ± 0.20^a
C+	1591 ± 0.35^a	0.60 ± 0.06^a	2.18 ± 0.19^b
T1	1610 ± 0.46^a	0.86 ± 0.04^b	4.22 ± 0.03^c
T2	1648 ± 0.48^a	0.90 ± 0.05^b	4.31 ± 0.02^c

Description: C−, negative control, no treatment; C+, positive control, topical ointment using Bioplacenton; T1, shrimp chitosan-based film; T2, BSFL exuviae chitosan-based film. Mean ± SE values followed by superscript letters (a,b,c) differing in the same column indicate significant differences (p-value < 0.05). Skin samples from rat wounds were collected on day 4, when one of the groups showed 100% wound closure

Figure 4: Wound closure images after treatment for 4 days. C−, negative control, no treatment; C+, positive control, topical ointment using bioplacenton; T1, shrimp chitosan-based film; T2, BSFL exuviae chitosan-based film. The films in groups T1 and T2 were applied directly to the wound bed and secured with a secondary dressing.

This significant increase in total protein content is consistent with an influx of plasma proteins, inflammatory mediators, and initial ECM deposition, a microenvironment often associated with successful early healing facilitated by chitosan-based materials [5]. In contrast, alginate-blended chitosan systems demonstrate limited protein accumulation owing to the swift resolution of edema [79].

Hydroxyproline concentrations, which indicate de novo collagen synthesis, exhibited intermediate levels in T2 (0.90 ± 0.05 µg/mL) and T1 (0.86 ± 0.04 µg/mL). These values were significantly lower than those in C− (1.25 ± 0.14 µg/mL) but higher than the positive control Bioplacenton (C+, 0.60 ± 0.06 µg/mL). The observed modulation of hydroxyproline levels indicates that BSFL chitosan may promote a more balanced early collagen synthesis than in the untreated control. While this pattern is consistent with a favorable early matrix environment, definitive conclusions regarding its long-term anti-fibrotic or scar-modulating effects require evaluation at later remodeling stages (14−21 days) using histological techniques [36], [80]. In contrast, plaque-like diabetic models employing nanochitosan carriers showed higher hydroxyproline levels following TGF-β1 overexpression [81], suggesting a milder and more physiological fibrogenic stimulus from the BSFL exuviae. The total DNA content, a marker of cellular proliferation, was significantly higher in T2 (4.31 ± 0.02 µg/mg) and T1 (4.22 ± 0.03 µg/mg) compared to C− (1.37 ± 0.20 µg/mg) and C+. This significant increase indicates a higher cellular density within the wound bed, which is consistent with enhanced cellular recruitment and/or proliferation, a common response to chitosan-based treatments attributed to their cationic nature and biocompatibility [44–54]. However, the specific cell types contributing to this increase were not characterized in this study. The reported values exceed those of gelatin-chitosan composites [28] and are in close agreement with the proliferative enhancement observed in stem-cell-laden chitosan hydrogels [82]. This indicates that the unique molecular properties of BSFL-derived chitosan may enhance its mitogenic efficacy in non-compromised acute wounds.

Overall, these results demonstrate that the BSFL exuviae-derived chitosan film significantly accelerated the early phases of wound repair, specifically hemostasis, inflammation, and proliferation, within 4 days in a rat model. The observed enhancements in wound closure, cellular proliferation (DNA), and modulated collagen synthesis (hydroxyproline) align with the known bioactive properties of chitosan. This study establishes a strong foundation for the efficacy of the material in acute wound management. However, its full impact on the subsequent remodeling phase and ultimate scar quality remains to be investigated in long-term studies [53–76]. Our findings align with those of Mahmoodi *et al.*, [81], whose curcumin-loaded chitosan nanoparticles resulted in 80% wound closure in diabetic rats by day 7, with similar kinetics based on anti-inflammatory effects. However, in the current study, the non-diabetic model showed faster healing rates. On the other hand, these previous studies contrast with Li *et al.*, [83], where unmodified chitosan films showed only 50% closure by day 5 in a rat burn model, demonstrating the superior efficacy of BSFL-derived materials. In agreement with Kathyayani *et al.*, [82], biopolymer chitosan composites reduced the size of the wounds by more than 70% in excised rat wounds, analogous to T2 but without bioconversion.

4 Conclusions

This study has demonstrated that black soldier fly larvae exuviae chitosan, when developed into films, significantly accelerates the early stages of wound healing in rats within 4 days, compared to conventional shrimp chitosan, ointments, and other treatments. Our primary findings indicated high extraction yields (chitin, 36.41–47.55%; chitosan, 33.97–48.66%), advantageous microstructural characteristics (porous nanofibers observed by SEM), and functional properties (such as amine-dominated FTIR spectra), along with enhanced in vivo results. By day 4, BSFL-chitosan significantly accelerated wound closure (2.62 ± 0.80 mm; p-value < 0.05 vs. controls) and was the only treatment that enhanced protein (1648 ± 0.48 μg/mg) and total DNA content (4.31 ± 0.02 μg/mg), indicating robust cellular proliferation in the wound bed. Furthermore, it uniquely reduced hydroxyproline levels (0.90 ± 0.05 μg/mL), suggesting an early modulatory effect on collagen synthesis that may help prevent excessive fibrosis. These results highlight BSFL exuviae as a novel, circular-economy biomaterial with promising antimicrobial and tissue-regenerative properties for wound care applications.

Certain study limitations are recognized. The short 4-day follow-up period provides no insights into long-term scarring or remodeling, the use of a non-diabetic rat model limits applicability to chronic wounds, and potential variability in exuviae composition could affect reproducibility. Another limitation is the absence of histological and gene expression analyses. While our biochemical (hydroxyproline and total DNA) and macroscopic (wound closure) data provide strong evidence for the efficacy of BSFL-chitosan films in accelerating early wound healing, they do not elucidate specific cellular mechanisms (fibroblast vs. keratinocyte proliferation, myofibroblast differentiation) or molecular regulation (Transforming Growth Factor-beta/TGF-β and COL1A1 expression). Future studies incorporating histology, immunohistochemistry, and qPCR are necessary to validate the inferred cellular activities and to fully understand the mechanism of action.

Recommendations for the future should include prolonged studies on diabetic or infected models, the integration of molecular investigations (such as Col I/III gene expression), studies on improving deacetylation of at least the nanochitosan variants, and human studies to assess the applicability and safety of the BSFL-chitosan product for the economically sustainable management of wounds. Comprehensive characterization of mechanical and physicochemical properties, as recommended by recent chitosan biomaterials literature, should be also prioritized in subsequent investigations to fully establish the translational potential of BSFL-chitosan films.

Acknowledgements

The authors express gratitude to the Ministry of Higher Education, Science and Technology, Indonesia (KEMDIKTISAINTEK) for financing this study (Contract number: NO:571/UN17.L1/HK/2025) and to all individuals who contributed to this research. We express our gratitude to the Department of Biology, Faculty of Mathematics and Natural Sciences, Mulawarman University, situated in Samarinda, East Kalimantan, Indonesia, for their many contributions.

Author Contributions

R.A.N.: conceptualization, investigation, reviewing and editing; R.A.: investigation, methodology, writing an original draft; H.K.: research design, data analysis; R.A.N, R.R, A.N.K, R.J.: conceptualization, data curation, writing, reviewing and editing, funding acquisition, project administration. All authors have read and agreed to the published version of the manuscript

Conflicts of Interest

The authors declare no conflict of interest.

Declaration of generative AI and AI-assisted technologies in the writing process

The authors utilized the QuillBot and Grammarly tools to enhance the language and readability of the manuscript. The Global Partnership on Artificial Intelligence (GPAI) application was used to generate the image of Figure 1, the manufacture of chitosan-based film.

Ethical Clearance

The animal study protocol was reviewed and approved by the Animal Ethics Committee of the Faculty of Medicine, Mulawarman University (Approval No: 17/01-24/22/2025). All procedures involving Wistar rats were conducted in strict accordance with the institution's guidelines for the care and use of

laboratory animals and are reported following the ARRIVE 2.0 guidelines.

References

[1] G. A. Varshan and S. K. R. Namasivayam, "A green chemistry principle for the biotransformation of fungal biomass derived chitosan into versatile nano scale materials with high biocompatibility and potential biological activities—A review," *BioNanoScience*, vol. 14, no. 1, pp. 4145–4166, 2024, doi: 10.1007/s12668-024-01564-0.

[2] S. Gul, Y. Karahan, O. B. Kurtur, and Y. Budama-Kilinc, *Cellulose, Chitin, and Chitosan Composite-Based Sustainable Biomaterials, in Sustainable Green Biomaterials*. Berlin, Germany: Springer, 2025, pp. 317–342, doi: 10.1007/978-3-031-79062-1_13.

[3] A. K. Maurya, "Sustainable food packaging: A brief review of chitosan-based materials," *International Journal of Science and Engineering Science Research*, vol. 1, no. 1, pp. 1–9, 2025, doi: 10.5281/zenodo.15731364.

[4] A. Li *et al.*, "Chitosan-based injectable hydrogel with multifunction for wound healing: A critical review," *Carbohydrate Polymers*, vol. 333, 2024, Art. no. 121952, doi: 10.1016/j.carbpol.2024.121952.

[5] S. M. Mawazi *et al.*, "Recent applications of chitosan and its derivatives in antibacterial, anticancer, wound healing, and tissue engineering fields," *Polymers*, vol. 16, no. 10, pp. 1–34, 2024, doi: 10.3390/polym16101351.

[6] M. Nasaj *et al.*, "Factors influencing the antimicrobial mechanism of chitosan action and its derivatives: A review," *International Journal of Biological Macromolecules*, vol. 277, no. 2, pp. 1–13, 2024, doi: 10.1016/j.ijbiomac.2024.134321.

[7] R. Cassano *et al.*, "Chitosan hemostatic dressings: Properties and surgical applications," *Polymers*, vol. 16, no. 13, pp. 1–11, 2024, doi: 10.3390/polym16131770.

[8] A. Haider *et al.*, "Chitosan as a tool for tissue engineering and rehabilitation: Recent developments and future perspectives–A review," *International Journal of Biological Macromolecules*, vol. 278, no. 1, 2024, Art. no. 134172, doi: 10.1016/j.ijbiomac.2024.134172.

[9] A. Ewais *et al.*, "Fully deacetylated chitosan from shrimp and crab using minimum heat input," *Egyptian Journal of Chemistry*, vol. 66, no. 2, pp. 321–337, 2023, doi: 10.21608/ejchem.2022.136694.6020.

[10] B. T. Iber *et al.*, "A review of various sources of chitin and chitosan in nature," *Journal of Renewable Materials*, vol. 10, no. 4, pp. 1–27, 2022, doi: 10.32604/JRM.2022.018142.

[11] B.-Q. Yuan *et al.*, "Physical and chemical characterization of chitin and chitosan extracted under different treatments from black soldier fly," *International Journal of Biological Macromolecules*, vol. 279, no. 2, pp. 1–12, 2024, doi: 10.1016/j.ijbiomac.2024.135228.

[12] H. González-Lara *et al.*, "Black soldier fly culture as a source of chitin and chitosan for its potential use in concrete: An overview," *Polymers*, vol. 17, no. 6, pp. 1–15, 2025, doi: 10.3390/polym17060717.

[13] R. A. Nugroho *et al.*, "Nutritive value, material reduction, biomass conversion rate, and survival of black solider fly larvae reared on palm kernel meal supplemented with fish pellets and fructose," *International Journal of Tropical Insect Science*, vol. 43, no. 4, pp. 1243–1254, 2023, doi: 10.1007/s42690-023-01032-4.

[14] R. A. Nugroho *et al.*, "Bioconversion of biowaste by black soldier fly larvae (*Hermetia illucens* L.) for dried larvae production: A life cycle assessment and environmental impact analysis," *F1000Research*, vol. 12, no. 1, pp. 1–9, 2023, doi: 10.12688/f1000research.132371.1.

[15] A. Santoso *et al.*, "Sustainability index analysis of the black soldier fly (*Hermetia illucens*) cultivation from food waste substrate," *Global Journal of Environmental Science and Management*, vol. 9, no. 4, pp. 851-870, 2023, doi: 10.22035/gjesm.2023.04.

[16] B. Fabian *et al.*, "Transformations of head structures during the larval development of the black soldier fly *Hermetia illucens* (Stratiomyidae, Diptera)," *Journal of Morphology*, vol. 286, no. 4, pp. 1–15, 2025.

[17] V. J. Kemboi *et al.*, "Biocontrol potential of chitin and chitosan extracted from black soldier fly pupal exuviae against bacterial wilt of tomato," *Microorganisms*, vol. 10, no. 1, pp. 1–13, 2022, doi: 10.3390/microorganisms10010165.

[18] E. Mirwandhono *et al.*, "Isolation and characterization of chitosan from black soldier fly exuviae," *IOP Conference Series: Earth and Environmental Science*, vol. 1362, no. 1, pp. 1–6, 2024.

[19] R. D. Sharma and P. Thangadurai, "Chitin from *Hermetia illucens* exuviae: A sustainable biopolymer yielding composition-defined functional oligomers with antioxidant cytoprotection," *International Journal of Biological Macromolecules*, vol. 3, no. 1, pp. 1–13, 2025, doi: 10.1016/j.ijbiomac.2025.149453.

[20] E. Fricke, R. Saborowski, and M. J. Slater, "Utility of by-products of black soldier fly larvae (*Hermetia illucens*) production as feed ingredients for Pacific Whiteleg shrimp (*Litopenaeus vannamei*)," *Journal of the World Aquaculture Society*, vol. 55, no. 4, pp. 1–16, 2024, doi: 10.1111/jwas.13070.

[21] A. Mannucci *et al.*, "From food waste to functional biopolymers: Characterization of chitin and chitosan produced from prepupae of black soldier fly reared with different food waste-based diets," *Foods*, vol. 13, no. 2, pp. 1–14, 2024, doi: 10.3390/foods13020278.

[22] A. Riofrio and H. Baykara., "Environmental impact of chitosan production from black soldier flies using life cycle assessment," *Materials Science Forum*, vol. 1108, no. 1, pp. 163–171, 2023, doi: 10.4028/fp-10p7DY.

[23] H. Teo *et al.*, "Antibacterial properties of chitosan isolated from the black soldier fly, *Hermetia illucens*," *Sains Malaysiana*, vol. 5, no. 12, pp. 3923–3935, 2022, doi: 10.17576/jsm-2022-5112-05.

[24] M. A. Cisternas and K. Varaprasad, *Chitosan-based Biomaterials for Hemostasis and Wound Healing*. Berlin, Heidelberg: Springer, 2025, pp. 367–401, doi: 10.1007/12_2024_179.

[25] V. Singh *et al.*, "Silk fibroin hydrogel: A novel biopolymer for sustained release of vancomycin drug for diabetic wound healing," *Journal of Molecular Structure*, vol. 1286, no. 1, 2023, Art. no. 135548, doi: 10.1016/j.molstruc.2023.135548.

[26] D. A. Sandakila *et al.*, "Ethanolic extract of black soldier fly (*Hermetia illucens* L.) larvae for wound healing in mice (*Mus musculus* L.)," *Aceh Journal of Animal Science*, vol. 9, no. 3, pp. 119-127, 2024, doi: 10.13170/ajas.9.3.42024.

[27] F. Akbari *et al.*, "In vitro and in vivo wound healing activity of *Astragalus floccosus* Boiss.(Fabaceae)," *Advances in Pharmacological and Pharmaceutical Sciences*, vol. 2022, no. 1, pp. 1–15, 2022, doi: 10.1155/2022/7865015.

[28] H. Yao *et al.*, "Fabrication and performance evaluation of gelatin/sodium alginate hydrogel-based macrophage and MSC cell-encapsulated paracrine system with potential application in wound healing," *International Journal of Molecular Sciences*, vol. 24, no. 2, pp. 1–15, 2023, doi: 10.3390/ijms24021240.

[29] N. I. Ibrahim *et al.*, "The effects of aqueous extract of *Labisia pumila* (Blume) Fern.-Vill. Var. Alata on wound contraction, hydroxyproline content and histological assessments in superficial partial thickness of second-degree burn model," *Frontiers in Pharmacology*, vol. 13, no. 1, pp. 1–15, 2022, doi: 10.3389/fphar.2022.968664.

[30] S. R. Tobat *et al.*, "Wound healing activity of phyllanthin-rich sub-fractions ointment: Isolated from meniran (P*hyllanthus niruri* L.) Leaf in experimental rats using hydroxyproline as biochemical marker," *Tropical Journal of Natural Product Research*, vol. 8, no. 7, pp. 1–15, 2024, doi: 10.26538/tjnpr/v8i7.15.

[31] L. Natrayan *et al.*, "Optimization process of potassium carbonate activated carbon through jute-based core materials by using artificial neural network with response surface methodology," *Adsorption Science & Technology*, vol. 2023, no. 1, pp. 1–14, 2023, doi: 10.1155/2023/8674382.

[32] N. Pragadish *et al.*, "A short review on AWJM of natural fibre reinforced composite materials," *Applied Mechanics and Materials*, vol. 912, no. 1, pp. 123–139, 2023, doi: 10.4028/p-bya4d7.

[33] P. Chankachang *et al.*, "Preparation and properties of chitosan/gelatin film containing capsaicinoid for hemostasis and antibacterial," *Colloids and Surfaces A: Physicochemical and Engineering Aspects*, vol. 694, no. 1, pp. 1–11, 2024, doi: 10.1016/j.colsurfa.2024.134078.

[34] C. N. Elangwe *et al.*, "A review on chitosan and cellulose hydrogels for wound dressings," *Polymers*, vol. 14, no. 23, pp. 1–17, 2022, doi: 10.3390/polym14235163.

[35] L. Elviri *et al.*, "Controlled local drug delivery strategies from chitosan hydrogels for wound healing," *Expert opinion on drug delivery*, vol. 14, no. 7, pp. 897–908, 2017, doi: 10.1080/17425247.2017.1247803.

[36] J. Shah *et al.*, "Recent advancements in chitosan-based biomaterials for wound healing," *Journal of Functional Biomaterials*, vol. 16, no. 2, pp. 1–18, 2025, doi: 10.3390/jfb16020045.

[37] M. K. Lagat *et al.*, "Antimicrobial activity of chemically and biologically treated chitosan prepared from black soldier fly (*Hermetia illucens*) pupal shell waste," *Microorganisms*, vol. 9, no. 12, pp. 1–15, 2021, doi: 10.3390/microorganisms9122417.

[38] D. I. Sánchez-Machado *et al.*, "Measurement of the degree of deacetylation in chitosan films by FTIR, 1H NMR and UV spectrophotometry," *MethodsX*, vol. 12, no. 1, pp. 1–7, 2024, doi: 10.1016/j.mex.2024.102583.

[39] H. Akram *et al.*, "Low solvothermal synthesis and characterization of hollow nanospheres molybdenum sulfide," *Journal of Nanoscience and Nanotechnology*, vol. 12, no. 8, pp. 6679–6685, 2012, doi: 10.1166/jnn.2012.4561.

[40] N. Akram *et al.*, "Fabrication and in vitro biological assay of thermo-mechanically tuned chitosan reinforced polyurethane composites," *Molecules*, vol. 28, no. 20, pp. 1–21, 2023, doi: 10.3390/molecules28207218.

[41] W. M. Abdeltwab *et al.*, "Antimicrobial effect of chitosan and nano-chitosan against some pathogens and spoilage microorganisms," *Journal of Advanced Laboratory Research in Biology*, vol. 10, no. 1, pp. 8–15, 2019, doi:

[42] M. Chandrasekaran, K. D. Kim, and S. C. Chun, "Antibacterial activity of chitosan nanoparticles: A review," *Processes*, vol. 8, no. 9, pp. 1–21, 2020, doi: 10.3390/pr8091173.

[43] T. Dai *et al.*, "Chitosan preparations for wounds and burns: antimicrobial and wound-healing effects," *Expert review of anti-infective therapy*, vol. 9, no. 7, pp. 857–879, 2011, doi: 10.1586/eri.11.59.

[44] R. Jayakumar *et al.*, "Biomaterials based on chitin and chitosan in wound dressing applications," *Biotechnology advances*, vol. 29, no. 3, pp. 322–337, 2011, doi: 10.1016/j.biotechadv.2011.01.005.

[45] A. Waśko *et al.*, "The first report of the physicochemical structure of chitin isolated from *Hermetia illucens*," *International Journal of Biological Macromolecules*, vol. 92, no. 1, pp. 316–320, 2016, doi: 10.1016/j.ijbiomac.2016.07.038.

[46] J. Wasko *et al.*, "Conjugates of chitosan and calcium alginate with oligoproline and oligohydroxyproline derivatives for potential use in regenerative medicine," *Materials*, vol. 13, no. 14, pp. 1–28, 2020, doi: 10.1016/j.ijbiomac.2016.07.038.

[47] H. El Knidri *et al.*, "Eco-friendly extraction and characterization of chitin and chitosan from the shrimp shell waste via microwave irradiation," *Process Safety and Environmental Protection*, vol. 104, no. 1, pp. 395–405, 2016, doi: 10.1016/j.psep.2016.09.020.

[48] N. G. Kandile *et al.*, "Extraction and characterization of chitosan from shrimp shells," *Open Journal of Organic Polymer Materials*, vol. 8, no. 3, pp. 33–42, 2018, doi: 10.4236/ojopm.2018.83003.

[49] A. J. da Silva Lucas *et al.*, "Extraction, physicochemical characterization, and morphological properties of chitin and chitosan from cuticles of edible insects," *Food chemistry*, vol. 343, no. 1, pp. 1–11, 2021, doi: 10.1016/j.foodchem.2020.128550.

[50] K. Mohan *et al.*, "Recent insights into the extraction, characterization, and bioactivities of chitin and chitosan from insects," *Trends in Food Science and Technology*, vol. 105, no. 1, pp. 17–42, 2020, doi: 10.1016/j.tifs.2020.08.016.

[51] Z. Sheng *et al.*, "Preparation, physicochemical properties and antimicrobial activity of chitosan from fly pupae," *Heliyon*, vol. 8, no. 10, pp. 1–8, 2022, doi: 10.1016/j.heliyon.2022.e11168 External Link.

[52] M. Aider, "Chitosan application for active bio-based films production and potential in the food industry," *LWT-Food Science and Technology*, vol. 43, no. 6, pp. 837–842, 2010, doi: 10.1016/j.lwt.2010.01.021.

[53] K. u. Rehman *et al.*, "Insect-derived chitin and chitosan: A still unexploited resource for the edible insect sector," *Sustainability*, vol. 15, no. 6, pp. 1–34, 2023, doi: 10.3390/su15064864.

[54] P. Feng *et al.*, "Chitosan-based functional materials for skin wound repair: Mechanisms and applications," *Frontiers in Bioengineering and Biotechnology*, vol. 9, no. 1, pp. 1–15, 2021, doi: 10.3389/fbioe.2021.650598.

[55] D. S. R. Rajkumar, K. Keerthika, and V. Vijayaragavan, "Chitosan-based biomaterial in wound healing: A review," *Cureus*, vol. 16, no. 2, pp. 1–18, 2024, doi: 10.7759/cureus.55193.

[56] A. Ehterami *et al.*, "In vitro and in vivo study of PCL/COLL wound dressing loaded with insulin-chitosan nanoparticles on cutaneous wound healing in rats model," *International Journal of Biological Macromolecules*, vol. 117, no. 1, pp. 601–609, 2018, doi: 10.1016/j.ijbiomac.2018.05.184.

[57] J. Natarajan *et al.*, "Nanostructured lipid carriers of pioglitazone loaded collagen/chitosan composite scaffold for diabetic wound healing," *Advances in Wound Care*, vol. 8, no. 10, pp. 499–513, 2019, doi: 10.1089/wound.2018.083.

[58] S. Dhivya, V. V. Padma, and E. Santhini, "Wound dressings–a review," *BioMedicine*, vol. 5, no. 4, pp. 24–28, 2015, doi: 10.7603/s40681-015-0022-9.

[59] J. Boateng and O. Catanzano, "Advanced therapeutic dressings for effective wound healing—A review," *Journal of Pharmaceutical Sciences*, vol. 104, no. 11, pp. 3653–3680, 2015, doi: 10.1002/jps.24610.

[60] G. Rivero, D. M. D. P. Pereira, C. Pablo, and G. A. Abraham, *Nanofibrous scaffolds for skin tissue engineering and wound healing applications, in Tissue engineering using ceramics and polymers*. Amsterdam, Netherlands: Elsevier, 2022, pp. 645–681, doi: 10.1016/B978-0-12-820508-2.00020-9

[61] M. A. Matica *et al.*, "Chitosan as a wound dressing starting material: Antimicrobial properties and mode of action," *International journal of molecular sciences*, vol. 20, no. 23, pp. 1–33, 2019, doi: 10.3390/ijms20235889.

[62] J. M. Budinčić *et al.*, "Exuviae of *Tenebrio molitor* larvae as a source of chitosan: Characterisation and possible applications," *Applied Sciences*, vol. 15, no. 17, pp. 1–25, 2025, doi: 10.3390/app15179285.

[63] J. R. B. Witono *et al.*, "Strategic advances in efficient chitin extraction from black soldier fly puparia: Uncovering the potential for direct chitosan production," *Polysaccharides*, vol. 6, no. 2, pp. 1–17, 2025, doi: 10.3390/polysaccharides6020026.

[64] M. Giani *et al.*, "*Hermetia illucens*-derived chitosan as a promising sustainable biomaterial for wound healing applications: development of sponge-like scaffolds," *International Journal of Biological Macromolecules*, vol. 304, no. 2, pp. 1–14, 2025, doi: 10.1016/j.ijbiomac.2025.140903.

[65] M. Triunfo *et al.*, "A comprehensive characterization of *Hermetia illucens* derived chitosan produced through homogeneous deacetylation," *International Journal of Biological Macromolecules*, vol. 271, no. 1, pp. 1–13, 2024, doi: 10.1016/j.ijbiomac.2024.132669.

[66] E. Mirwandhono *et al.*, "Isolation and characterization of chitosan from black soldier fly exuviae," *IOP Conference Series: Earth and Environmental Science*, vol. 1362, no. 1, pp. 1–6, 2024, doi: 10.1088/1755-1315/1362/1/012013.

[67] L. Queiroz *et al.*, "Physico-chemical and colloidal properties of protein extracted from black soldier fly (*Hermetia illucens*) larvae," *International Journal of Biological Macromolecules*, vol. 186, no. 1, pp. 714–723, 2021, doi: 10.1016/j.ijbiomac.2021.07.081.

[68] S. A. Siddiqui *et al.*, "The potential of chitin and chitosan from dead black soldier fly (BSF) (*Hermetia illucens*) for biodegradable packaging material – A critical review," *Process Safety and Environmental Protection*, vol. 189, no. 1, pp. 1342–1367, 2024, doi: 10.1016/j.psep.2024.06.108.

[69] A. Marangon *et al.*, "Chitin extracted from black soldier fly larvae at different growth stages," *Polymers (Basel)*, vol. 16, no. 20, pp. 1–12, 2024, doi: 10.3390/polym16202861.

[70] D. Purkayastha and S. Sarkar, "Physicochemical structure analysis of chitin extracted from pupa exuviae and dead imago of wild black soldier fly (*Hermetia illucens*)," *Journal of Polymers and the Environment*, vol. 28, no. 2, pp. 445–457, 2020, doi: 10.1007/s10924-019-01620-x.

[71] E. Mirwandhono *et al.*, "Isolation and characterization of chitosan from black soldier fly exuviae," *IOP Conference Series: Earth and Environmental Science*, vol. 1362, no. 1, pp. 1–6, 2024, doi: 10.1088/1755-1315/1362/1/012013.

[72] M. Triunfo *et al.*, "Characterization of chitin and chitosan derived from *Hermetia illucens*, a further step in a circular economy process," *Scientific Reports*, vol. 12, no. 1, pp. 1–17, 2022, doi: 10.1038/s41598-022-10423-5.

[73] D. Archana, J. Dutta, and P. Dutta, "Evaluation of chitosan nano dressing for wound healing: Characterization, in vitro and in vivo studies," *International Journal of Biological*

Macromolecules, vol. 57, no. 1, pp. 193–203, 2013, doi: 10.1016/j.ijbiomac.2013.03.002.

[74] H. Bai *et al.*, "Regulation of inflammatory microenvironment using a self-healing hydrogel loaded with BM-MSCs for advanced wound healing in rat diabetic foot ulcers," *Journal of Tissue Engineering*, vol. 11, no. 1, pp. 1–13, 2020, doi: 10.1177/2041731420947242.

[75] C. Viezzer *et al.*, "A new waterborne chitosan-based polyurethane hydrogel as a vehicle to transplant bone marrow mesenchymal cells improved wound healing of ulcers in a diabetic rat model," *Carbohydrate Polymers*, vol. 231, no. 1, pp. 1–10, 2020, doi: 10.1016/j.carbpol.2019.115734.

[76] M. S. Al-saggaf, "Formulation of insect chitosan stabilized silver nanoparticles with propolis extract as potent antimicrobial and wound healing composites," *International Journal of Polymer Science*, vol. 2021, no. 1, pp. 1–9, 2021, doi: 10.1155/2021/5578032.

[77] C. S. Liew *et al.*, "Chitin and chitosan production from black soldier fly larvae (*Hermertia illucens*) as bioresource: Current progress, applications, challenges and way forwards," *Waste and Biomass Valorization*, vol. 17, no. 1, pp. 1–12, 2026, doi: 10.1007/s12649-025-03175-6.

[78] X. Che *et al.*, "Application of chitosan-based hydrogel in promoting wound healing: A review," *Polymers*, vol. 16, no. 3, pp. 1–20, 2024, doi: 10.3390/polym16030344.

[79] A. Haider *et al.*, "Chitosan as a tool for tissue engineering and rehabilitation: Recent developments and future perspectives – A review," *International Journal of Biological Macromolecules*, vol. 278, no. 1, pp. 1–13, 2024, doi: 10.1016/j.ijbiomac.2024.134172.

[80] S. Pramanik *et al.*, "Chitosan alchemy: transforming tissue engineering and wound healing," *RSC advances*, vol. 14, no. 27, pp. 19219–19256, 2024, doi: 10.1039/d4ra01594k.

[81] M. Mahmoodi *et al.*, "Evaluation of gene expression levels in diabetic rat skin wound healing treated with chitosan/curcumin nanoparticles-loaded sodium alginate/chitosan hydrogels," *International Journal of Biological Macromolecules*, vol. 324, no. 1, pp. 1–14, 2025, doi: 10.1016/j.ijbiomac.2025.147220.

[82] D. Kathyayani *et al.*, "Insights into the physicochemical characteristics and miscibility of chitosan/polypeptide blends: Promising material for wound healing in sprague–dawley rats," *ACS Biomaterials Science & Engineering*, vol. 10, no. 9, pp. 5807–5821, 2024, doi: 10.1021/acsbiomaterials.4c01123.

[83] Y. Li *et al.*, "Therapeutic effects of EGF-modified curcumin/chitosan nano-spray on wound healing," *Regenerative Biomaterials*, vol. 8, no. 2, pp. 1–9, 2021, doi: 10.1093/rb/rbab009.